Determination of the frequency response of higher-order RC filters

Kenneth Domingo, Rhei Joven Juan, and Rene Principe Jr.

National Institute of Physics, University of the Philippines, Diliman, Quezon City

Abstract

We extend the frequency response analysis of higher-order RC filters with Sallen-Key topology and Multiple feedback topology. Bode plots in terms of gain has exhibited the appropriate low-pass and high-pass frequency response yet it failed to match the theoretical pass band gain of 6 dB as well as the roll-on/roll-off rate magnitude of 40 dB. In our experiment, pass band gain were consistently lower at around -30 dB for three out of four configurations, and the slope behaved like a first-order at a magnitude of 20 dB for both roll-on and roll-off. Errors may be due to the non-idealities in our components as well as the choice for our RC values.

Keywords: frequency response, Bode plot, transfer function.

1 Introduction

From a previous exeperiment we were able to find out that The frequency response of a device can be shown through plotting the gain and phase over a wide range of operating frequencies in a semi-logarithmic scaled Bode plot [1]. The gain and phase can be calculated using (1)-(2):

$$\text{Gain(dB)} = 20 \log \frac{V_{out}}{V_{in}} \tag{1}$$

$$\phi = -\arctan(2\pi f RC) \tag{2}$$

where V_{in} and V_{out} are the magnitude of the input and output signals respectively and f is the operating frequency at which the aforementioned values were recorded. In this experiment, we look into the frequency response for higher-order RC filters, in this case the second-order active filters.

For a second-order filter, there are two topologies used, specifically the Sallen-Key and Multiple Feedback (MFB) topology [2]. The Sallen-Key topology, also known as voltage control voltage source, was first introduced by R.P. Sallen and E.L. Key back in 1955. It is one of the most widely used topologies because it shows the least dependence of filter performance on the performance of the operational amplifier [3], in which the minimum gain bandwidth does not limit the performance of the filter, like in an integrator. The general circuit diagram is shown in figure 1 and its transfer function for both high-pass and low-pass filters are shown in equations 3 and 4.

$$G(s) = \frac{H \dfrac{1}{R_1 R_2 C_1 C_2}}{s^2 + s\left[\left(\dfrac{1}{R_1} + \dfrac{1}{R_2}\right)\dfrac{1}{C_1} + \dfrac{1-H}{R_2 C_2}\right] + \dfrac{1}{R_1 R_2 C_1 C_2}} \tag{3}$$

$$G(s) = \frac{Hs^2}{s^2 + s\left[\frac{\frac{C_2}{R_2} + \frac{C_1}{R_2} + (1-H)\frac{C_2}{R_1}}{C_1 C_2}\right] + \frac{1}{R_1 R_2 C_1 C_2}} \tag{4}$$

The multiple feedback (MFB) topology on the other hand creates an inverting second-order stage, with circuit diagram shown in figure 2 and transfer functions shown in equations 5 and 6.

$$G(s) = \frac{-H\frac{1}{R_1 R_3 C_2 C_5}}{s^2 + s\frac{1}{C_2}\left(\frac{1}{R_1} + \frac{1}{R_3} + \frac{1}{R_4}\right) + \frac{1}{R_3 R_4 C_2 C_5}} \tag{5}$$

$$G(s) = \frac{-s^2\frac{C_1}{C_4}}{s^2 + s\left(\frac{C_1 + C_3 + C_4}{C_3 C_4 R_5}\right) + \frac{1}{R_2 R_5 C_3 C_4}} \tag{6}$$

For both topologies, the gain H is given by:

$$H = 1 + \frac{R_4}{R_3} \tag{7}$$

2 Methodology

By setting a specific cut-off frequency by choosing the resistors and capacitors used in the circuit, the Sallen-Key filter and multiple feedback circuits for both high-pass and low-pass were constructed. The Bode plots were obtained by recording the voltage in and voltage out at different frequencies. The transfer function of the system was then estimated using the Bode plot and compared to the analytic transfer function computed from the given circuit diagrams.

3 Results and Discussion

3.1 Sallen-Key topology

3.1.1 Low-pass filter

The schematic of a Sallen-Key filter is shown in Figure 1. In order for this circuit to behave as a low-pass filter, elements `Z1` and `Z2` are set as resistors, while elements `Z3` and `Z4` are set as capacitors. For all the succeeding circuits, all resistors and capacitors are set fixed at 1 Ω and 22 μF, respectively. With a fixed value of $V_{in} = 5$ V, the output voltage readings were recorded manually. The phase readings were no longer recorded due to erroneous readings from the oscilloscope. As a result, only the magnitude Bode plots were plotted. In order to determine the experimental Bode plot, the obtained magnitude data were fit with an equation of the form of (3) using nonlinear least-squares method, with the gain H, resistances R, and capacitances C as elements of the parameter vector. From the plot, it can be observed that the experimental has a pass band gain of approximately -30 dB, which exhibits a great disparity from the analytically calculated 6 dB. The theoretical and experimental are in agreement at the cutoff frequency of $\omega_c = 4.5 \times 10^4$ rad/s, but behave very differently onwards. The experimental rolls-off at a rate of -20

dB/decade as opposed to the expected −40 dB/decade. Hence, the system behaves more like a first-order RC filter. The experimental and theoretical transfer functions are:

$$G_{\text{expt}}^{\text{SKLP}}(s) = \frac{2.33 \times 10^{15}}{s^2 + 1.00 \times 10^{12} s + 7.10 \times 10^{16}} \tag{8}$$

$$G_{\text{theo}}^{\text{SKLP}}(s) = \frac{4.13 \times 10^{9}}{s^2 + 4.55 \times 10^{4} s + 2.07 \times 10^{9}} \tag{9}$$

3.1.2 High-pass filter

In order for Figure 1 to behave as a high-pass filter, all settings as before are maintained, except the roles of the `Z` elements are switched, and the same procedure follows. The experimental data was fit with an equation of the form of (4). From Figure 4, it can be observed that the theoretical and experimental no longer agree with the cutoff frequency (it should be the same as in the Sallen-Key low-pass). The experimental cutoff is much lower and roll-on increases at a rate +20 dB/decade, as opposed to the theoretical +40 dB/decade. The pass band gain settles at −34 dB, as opposed to the expected 6 dB. The system, once again, behaves like a first-order RC filter. The experimental and theoretical transfer functions are:

$$G_{\text{expt}}^{\text{SKHP}}(s) = \frac{2.11 \times 10^{-2} s^2}{s^2 + 64.84 s + 1051.21} \tag{10}$$

$$G_{\text{theo}}^{\text{SKHP}}(s) = \frac{2 s^2}{s^2 + 4.55 \times 10^{4} s + 2.07 \times 10^{9}} \tag{11}$$

3.2 Multiple feedback topology

3.2.1 Low-pass filter

The schematic of a multiple feedback low-pass filter is shown in Figure 2. All settings were maintained as before and the same procedure was followed. The experimental data was initially fit with an equation of the form of (5). However, the best-fit curve was plotted too far from the data points. Instead, the data was fit to a second-order transfer function of the form

$$G(s) = \frac{A}{Bs^2 + Cs + D} \tag{12}$$

where A, B, C, and D are constants and are elements of the curve-fitting parameter vector. The results plotted in Figure 5 show, once again, first-order system behavior. The pass band gain of −3 dB is now closer to the expected 6 dB, but the roll-off is still −20 dB/decade, as opposed to the expected −40 dB/decade. The experimental and theoretical transfer functions are:

$$G_{\text{expt}}^{\text{MFLP}}(s) = \frac{0.04}{s^2 + 475.63 s + 0.02} \tag{13}$$

$$G_{\text{theo}}^{\text{MFLP}}(s) = \frac{-4.13 \times 10^{9}}{s^2 + 1.36 \times 10^{5} s + 2.07 \times 10^{9}} \tag{14}$$

3.2.2 High-pass filter

In order for Figure 2 to behave as a high-pass filter, the resistors and capacitors simply need to be interchanged, and the same procedure follows. The experimental data was initially fit with an equation of the form (6). However, the best-fit curve was, once again, too far from the data points. Instead, the data was fit with a second-order function of the form

$$G(s) = \frac{As^2}{Bs^2 + Cs + D} \tag{15}$$

where A, B, C, and D are constants and are elements of the curve-fitting parameter vector. The results shown in Figure 6 show that the pass band gain settles at -28 dB, as opposed to the expected 6 dB, and the roll-on rate is $+20$ dB/decade as opposed to the ideal $+40$ dB/decade. The system once again behaves like a first-order filter. The experimental and theoretical transfer functions are:

$$G^{\text{MFHP}}_{\text{expt}}(s) = \frac{0.04s^2}{s^2 + 475.63s + 0.02} \tag{16}$$

$$G^{\text{MFHP}}_{\text{theo}}(s) = \frac{-s^2}{s^2 + 1.36 \times 10^5 s + 2.07 \times 10^9} \tag{17}$$

The consistent results shown above indicates the non-idealities that may be exhibited by the electrical components, which cause lower than expected gain, as well as lower than expected roll-on/roll-off rate.

4 Conclusions

Only the bode plots in terms of gain were analyzed since we deemed that the oscilloscope used reads inaccurate phase values. From the plot, the experimental w_c agreed with the theoretical calculation for the low-pass Sallen-Key filter, while the w_c for the high-pass Sallen-Key filter was nowhere close to the same theoretical value of 4.5×10^4 rad/s. Both low-pass and high-pass Sallen-Key filters had pass band gain way off the analytically calculated value of 6 dB as our experiment returned pass band gains of -30 dB and -34 dB respectively. In the multiple freedback circuit topologies, only the low-pass filter returned a pass band gain relatively closer to the expected 6 dB as we experimentally recorded it to be -3 dB, while the high-pass counterpart had another way off value of -28 dB.

For both the Sallen-Key topology and Multiple feedback topology, the experimental bode plots (gain) turned out to have lower roll-on/roll-off rates at a magnitude of 20 dB/decade compared to the theoretical roll-on/roll-off magnitude rate of 40 dB/decade. We then estimated the transfer functions of all systems from the experimental bode plot and compared it to the analytically generated transfer functions. These disparities in our experimental results can be summarized to the observation that all of our higher-order RC filters behaved like a first-order filter as suggested by the lower pass band gain and roll-on/roll-off rates. These non-idealities were consistent throughout all of our results hence the error can be attributed to the electrical components used, as well as the choice of our resistance and capacitance values for the RC components.

References

[1] Electronics Tutorials. Frequency Response. Retrieved 21 April 2019 from https://www.electronics-tutorials.ws/amplifier/frequency-response.html/

[2] Texas Instruments. Activer Filter Design Techniques. *Op Amps for Everyone*. Dallas, Texas (2001).

[3] Zumnahlen, Hank, editor, 2008. Analog Filters. *Linear Circuit Design Handbook*, Newnes, ISBN 978-0-7506-8703-4.

[4] User: Inductiveload. (2009). A diagram of the generic Sallen-Key filter [Own work, public domain]. Retrieved 21 April 2019, from *Wikimedia Commons*: https://commons.wikimedia.org/wiki/File:Sallen-Key_Generic_Circuit.svg.

[5] User: PAR. (2006). Diagram of a multiple feedback topology electronic filter circuit [Own work, public domain]. Retrieved 21 April 2019, from *Wikimedia Commons*: https://commons.wikimedia.org/wiki/File:MFB_Topology.png.

Appendix

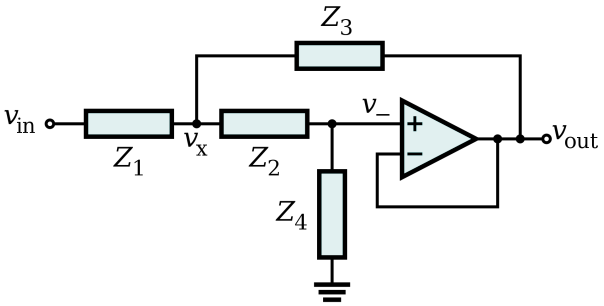

Figure 1: Schematic of a generic Sallen-Key filter [4].

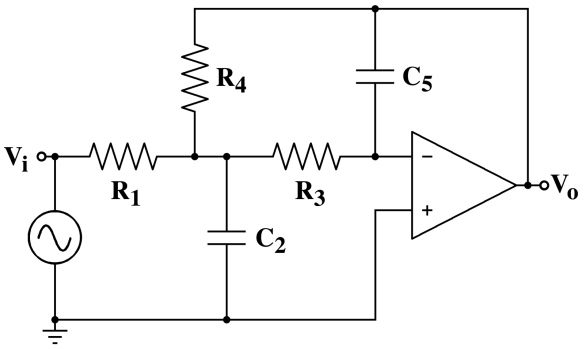

Figure 2: Schematic of a multiple feedback filter [5].

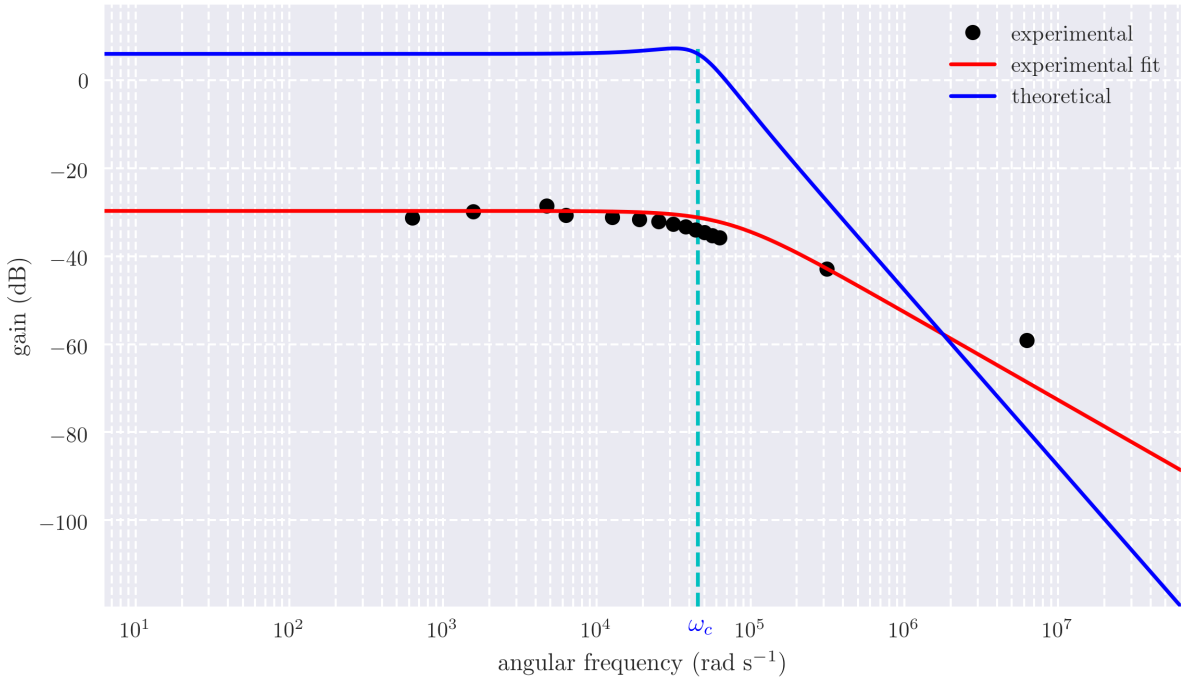

Figure 3: Frequency response of a Sallen-Key low-pass filter.

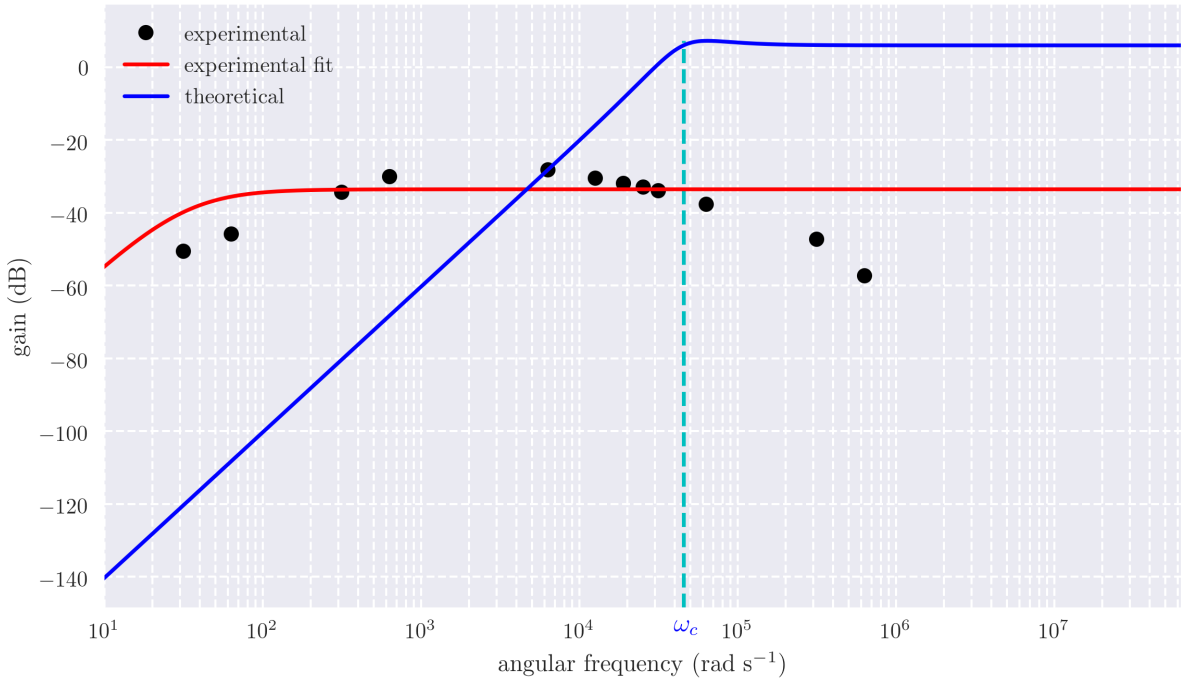

Figure 4: Frequency response of a Sallen-Key high-pass filter.

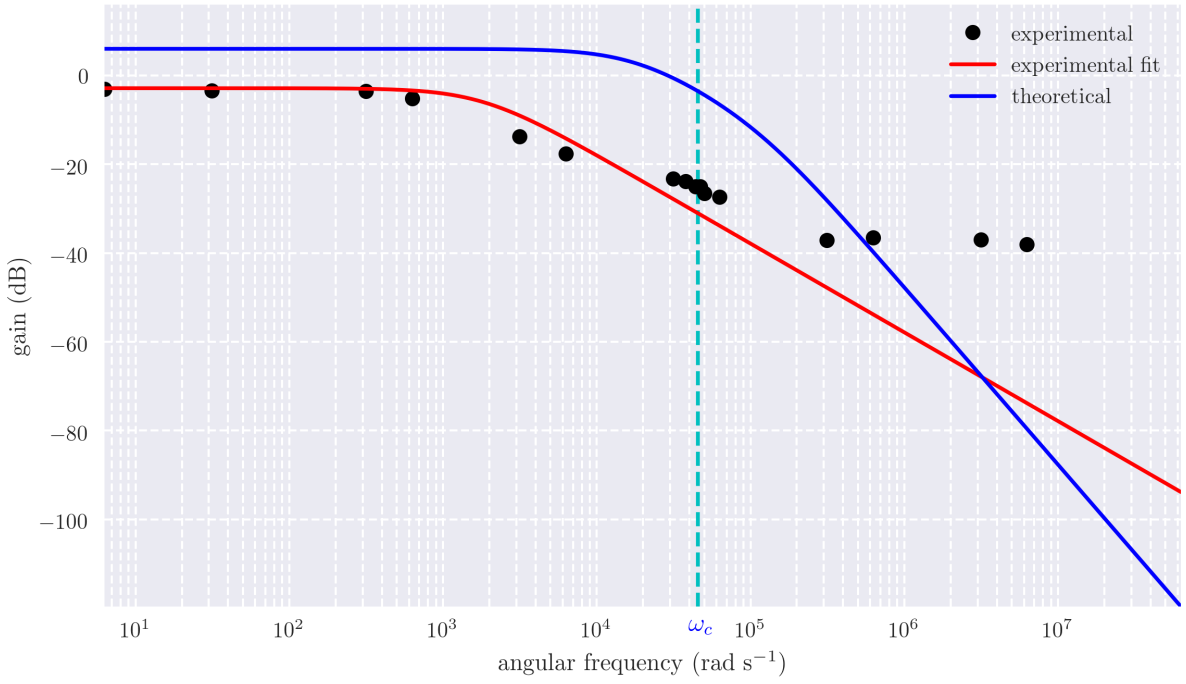

Figure 5: Frequency response of a multiple feedback low-pass filter.

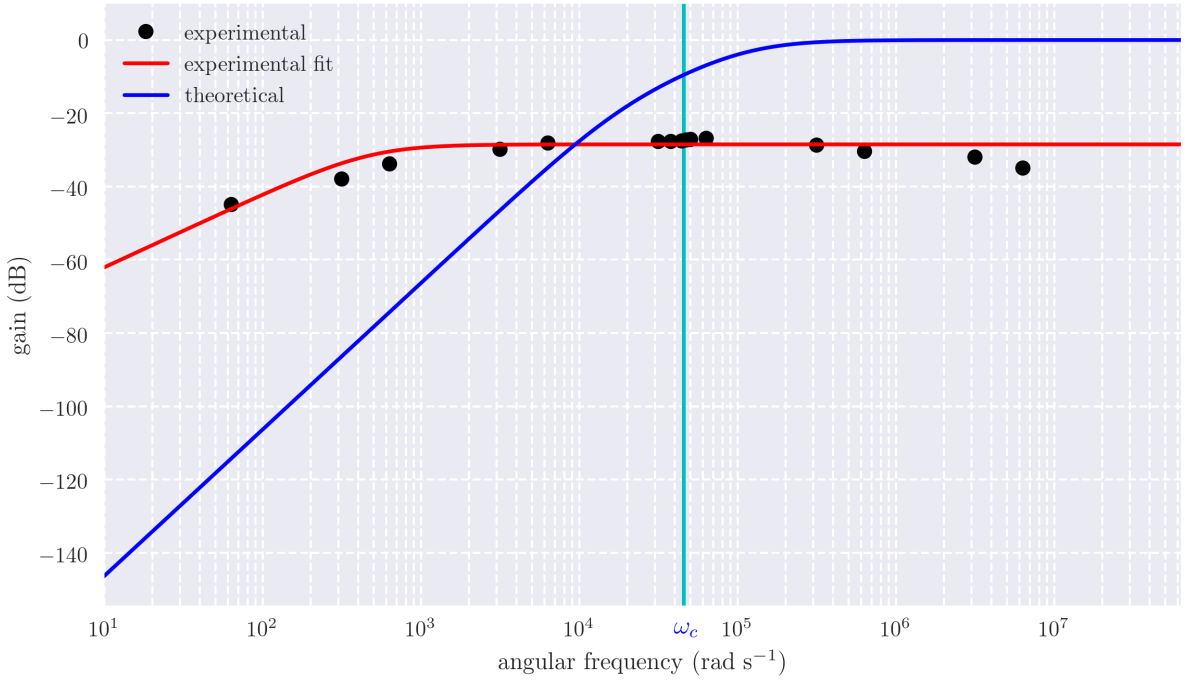

Figure 6: Frequency response of a multiple feedback high-pass filter.